Numerical modeling of contaminant transport resulting from dissolution of a coal-tar pool in an experimental aquifer

Kenneth Y. Lee · Johannes Khinast · Jung-Hoon Kim

Abstract A previously developed two-dimensional numerical model is further developed for simulating the transport of dissolved contaminants originating from dissolution of a coal tar pool in a stratified, saturated porous medium. The model is used to simulate contaminant transport resulting from a rectangular-shaped coal-tar-pool dissolution experiment conducted in a large-scale experimental aquifer. The experimental porous medium consists of two sand strata, a high-hydraulic-conductivity upper stratum and a low-hydraulic-conductivity bottom stratum. The experiment was conducted to a time of 354 days and the groundwater velocity was changed several times within this duration. Model simulations show good agreement against observed contaminant concentrations, and simulations show that dissolved solute below the pool migrated deeper into the bottom stratum as compared to the upper stratum. Furthermore, simulations also suggest that contaminant concentrations in the lower stratum never reached quasi steady-state during the experimental time frame.

Résumé Un modèle 2D numérique construit précédemment est développé plus en avant pour simuler le transport de contaminants dissous originaires de la dissolution d'un gisement de goudron de houille dans un milieu poreux stratifié et saturé. Le modèle est utilisé pour simuler le transport de contaminant résultant d'une expérience de dissolution d'un gisement rectangulaire de goudron de houille, conduite dans un aquifère expérimental à large échelle. Le milieu poreux expérimental consiste en deux strates de sables: une à forte conductivité hydraulique dans la strate la plus élevée, et une à basse conductivité hydraulique dans la strate la plus basse. L'expérience a été conduite durant 354 jours et la vitesse de l'eau souterraine a variée plusieurs fois durant cette période. Les simulations du modèle montrent une bonne concordance avec les concentrations observées en contaminant; elles montrent aussi que le soluté dissout sous le gisement descend plus profondément dans la strate la plus basse, comparée à la strate la plus haute. De plus, les simulations suggèrent également que les concentrations en contaminant dans la strate la plus basse n'atteignent jamais un état quasi-permanent durant le temps d'expérimentation.

Resumen Un modelo numérico en dos dimensiones desarrollado previamente ha sido rediseñado para simular el transporte de contaminantes disueltos cuyo origen es la disolución de una balsa de alquitrán en un medio estratificado, saturado y poroso. El modelo se ha utilizado para simular el transporte de contaminantes resultante de la disolución de una balsa de alquitrán de forma rectangular en un acuífero experimental a gran escala. El medio poroso experimental consiste en dos estratos de arena, uno superior con una conductividad alta y otro inferior con baja conductividad. El experimento se llevó a cubo durante 354 días y la velocidad del agua subterránea se cambió varias veces durante este tiempo. Las simulaciones del modelo presentan una buena correlación con las concentraciones observadas de contaminante, y muestran que el soluto disuelto bajo la balsa migró más profundamente dentro del estrato inferior comparativamente con el estrato superior. Además, las simulaciones también apuntaban a que las concentraciones de contaminante en el estrato inferior no alcanzaban nunca el estado casi estacionario durante el tiempo de experimentación.

Keywords Coal tar · Solute transport · Groundwater protection · Contamination · Numerical modeling

Received: 7 August 2005 / Accepted: 30 November 2006
Published online: 5 January 2007

K. Y. Lee (✉)
Department of Civil Engineering,
West Virginia University Institute of Technology,
Montgomery, WV 25136, USA
e-mail: Kenneth.Lee@mail.wvu.edu
Tel.: +1-304-4423373

J. Khinast
Department of Chemical and Biochemical Engineering,
Rutgers, The State University of New Jersey,
Piscataway, NJ 08854, USA

J.-H. Kim
Department of Civil and Environmental Engineering,
Rutgers, The State University of New Jersey,
Piscataway, NJ 08854, USA

 DOI 10.1007/s10040-006-0144-y

Introduction

Groundwater contamination from coal tar is a widespread environmental problem. In general, coal tar is a multicomponent dense nonaqueous phase liquid (DNAPL) consisting of a variety of compounds. A typical coal tar contains a complex mixture of BTEX (benzene (BEN), toluene (TOL), ethylbenzene (ETH), and xylenes (PXY, OXY)) compounds, PAH (polycyclic aromatic hydrocarbon) compounds, asphaltenes, and other soluble and insoluble compounds (Dong et al. 2004). Coal tar is a very persistent subsurface contaminant source because its compounds have low aqueous solubility (and even lower equilibrium aqueous solubility). Aquifer contamination from a coal-tar source may last for decades, or even centuries or longer (Eberhardt and Grathwohl 2002; Lee 2004).

It is important to understand the multicomponent coal-tar dissolution behavior in order to predict solute fate and transport. This knowledge can help environmental scientists and engineers to estimate the duration and extent of aquifer contamination, and to assess groundwater quality impacts. One unique phenomenon associated with PAH compounds is that they are generally solid in their pure state at ambient conditions, and only exist as a nonaqueous phase liquid (NAPL) when a compound's solid to liquid reference fugacity ratio is greater than the compound's nonaqueous phase mole fraction (Brown et al. 1999). As a result, some PAH compounds within a dissolving coal-tar source may solidify as their mole fraction within the mixture changes with time (Peters et al. 1997; Lee 2004).

For a dissolving coal-tar source, the resulting multicomponent plume is effectively separated into a series of single component plumes, each of which may exhibit distinct sorptive characteristics (King and Barker 1999). It is generally acknowledged that many coal-tar components are subject to biodegradation. However, biodegradation may not significantly alter the dissolution time scale of a coal-tar source (Mueller et al. 1989). It should also be noted that carcinogenicity and toxicity effects vary for different coal-tar components (Dabestani and Ivanov 1999; Loibner et al. 2004). Therefore, environmental scientists and engineers might only be interested in the fate and transport of a few selected, or a group of dissolved coal-tar components (Lee 2004). For example, a group of only 16 PAH compounds (out of more than one hundred different PAH compounds) are prioritized by the US Environmental Protection Agency (Loibner et al. 2004).

Due to the large number of components and the complexity of component interactions within the coal-tar source, it is difficult to experimentally study the dissolution behavior of individual components in the laboratory. Furthermore, changes in coal-tar dissolution behavior may take years or longer to observe. Eberhardt and Grathwohl (2002) conducted a coal-tar pool/blob dissolution experiment in a rectangular-shaped experimental aquifer. These researchers did not observe any changes in dissolution rate within the experimental time duration of 354 days. Lee and Chrysikopoulos (2006) conducted a two-component DNAPL pool dissolution experiment in a homogeneous experimental aquifer. These researchers were able to observe changes in dissolution behavior of one component within a reasonable amount of experimental time by using a very small initial mole fraction for that component.

In this research, a previously developed two-dimensional multicomponent solute transport numerical model (Lee and Chrysikopoulos 1998) is further developed for describing contaminant transport resulting from dissolution of a coal-tar pool in a stratified, saturated porous medium. The model is used to simulate and describe the previously mentioned coal-tar pool dissolution experiment conducted by Eberhardt and Grathwohl (2002).

Model development

Equilibrium aqueous phase solubility

For a dissolving multicomponent coal-tar pool, the time-dependent equilibrium aqueous phase concentration of each component, $C_p^w(t)$, at the coal-tar/water interface can be described by (Brown et al. 1999)

$$C_p^w(t) = \frac{C_p^s X_p(t)}{\left(f^{\mathrm{S}}/f^{\mathrm{L}}\right)_p} \tag{1}$$

where subscript p is the component indicator; C_p^s is the aqueous saturation concentration (solubility) of pure component p; $\left(f^{\mathrm{S}}/f^{\mathrm{L}}\right)$ is the solid to liquid reference fugacity ratio; $X(t)$ is the time-dependent nonaqueous phase mole fraction. It should be noted that Eq. (1) assumes ideal molecular behavior in the nonaqueous phase. Eberhardt and Grathwohl (2002) have demonstrated that this assumption is valid for the coal tar used in their dissolution experiment.

For a coal-tar pool trapped at the interface between two distinct subsurface strata, dissolution will occur simultaneously above and below the pool. However, the dissolution rate in each stratum may vary depending on the properties and flow characteristics of each stratum. As the coal-tar pool dissolves, the source volume, $V(t)$, decreases over time and may be estimated using (Lee 2004)

$$V(t) = \theta A(t) d(t) = \sum_{p=1}^{P} \frac{M_p(t)(\mathrm{molwt})_p}{\rho_p} \tag{2}$$

where θ is the porosity of the porous medium; $A(t)$ is the pool/water interfacial area at time t; $d(t)$ is the pool thickness at time t; P is the total number of components in the coal-tar pool; ρ is the density; and $M_p(t)$ is the number of moles of component p in the coal-tar pool source at time t defined as (Chrysikopoulos and Lee 1998)

$$M_p(t) = M_p(0) - \sum_{m=1}^{m_f} \frac{\left(\overline{k}_p^{\mathrm{T}}(m\Delta t) + \overline{k}_p^{\mathrm{B}}(m\Delta t)\right) C_p^w(m\Delta t) A(m\Delta t)\theta\Delta t}{(\mathrm{molwt})_p} \tag{3}$$

DOI 10.1007/s10040-006-0144-y

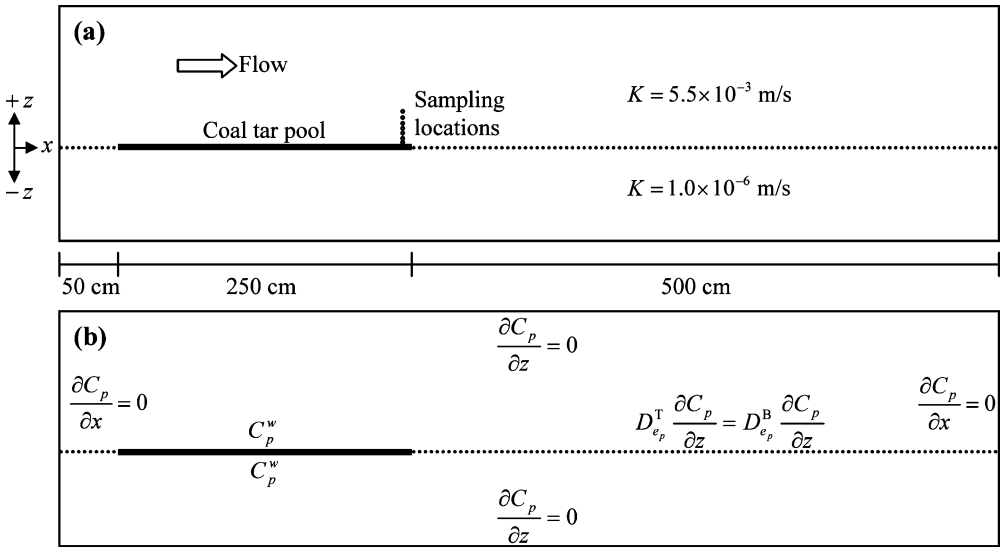

Fig. 1 **a** Simplified cross-section diagram of the experimental aquifer and **b** the numerical domain with boundary conditions

where $M_p(0)$ is the initial number of moles of component p within the pool source; m is a summation index; m_f indicates the total number of numerical time steps; Δt is the duration of each numerical time step; and $\overline{k}^{\mathrm{T}}(t)$, $\overline{k}^{\mathrm{B}}(t)$, are the time dependent average (or overall) mass transfer coefficient applicable at the top and bottom pool/water interface, respectively. It should be noted that Eq. (2) assumes that the density of a component is identical in both the solid and the nonaqueous liquid phase, and that the formation of solids does not significantly alter the overall coal-tar pool volume or interfere with the overall pool/water interfacial-mass-transfer process.

The usage of Eqs. (2) and (3) require a comprehensive identification of all coal-tar components, as well as initial mole fraction data for each component. Without this information, these equations cannot estimate the mole fraction of each component as a function of time, and are consequently unable to estimate the time at which solidification occurs. Due to the large number and complexity of compounds in a typical coal tar, it is difficult to identify all compounds using existing analytical techniques. As a result, coal-tar analysis reported in literature often contains a nonidentifiable fraction (e.g., Eberhardt and Grathwohl 2002; Tiruta-Barna et al. 2006). Consequently, Eqs. (2) and (3) are not used in this study.

Multicomponent solute transport

The two-dimensional transient contaminant transport from a dissolving multicomponent NAPL pool in a homogeneous saturated porous medium is governed by the following partial differential equation (Lee and Chrysikopoulos 1998)

$$R_p \frac{\partial C_p(t,x,z)}{\partial t} = D_{x_p} \frac{\partial^2 C_p(t,x,z)}{\partial x^2} + D_{z_p} \frac{\partial^2 C_p(t,x,z)}{\partial z^2} - U_x \frac{\partial C_p(t,x,z)}{\partial x} - \lambda_p R_p C_p(t,x,z) \quad (4)$$

where R is the dimensionless retardation factor; C is the aqueous phase solute concentration; x, z are the spatial coordinates in the longitudinal and vertical directions, respectively; $D_x = \alpha_x U_x + D_e$, $D_z = \alpha_z U_x + D_e$ are the hydrodynamic dispersion coefficients in the x and z directions, respectively; α_x, α_z are the dispersivity coefficients in the x and z directions, respectively; U_x is the groundwater velocity; $D_e = D/\tau^*$ is the effective molecular diffusion coefficient; D is the molecular diffusion coefficient in water; τ^* ($\tau^* \geq 1$) is the tortuosity; and λ is a first-order decay constant.

Coal-tar pool dissolution experiment

The coal-tar pool dissolution experiment was conducted by Eberhardt and Grathwohl (2002). The experiment was carried out in a 16-m long, 1-m wide, and 3-m high tank. However, only half of the tank length, or 8 m, was used for this experiment. Figure 1a shows a simplified cross-section diagram of the experimental aquifer showing the location of the coal-tar pool along the x axis. Note that the figure is not scaled in the vertical direction. It should also be noted that in this modeling study, the primary focus is on the dissolution of the coal-tar pool, and therefore does not take into account dissolution results from the coal-tar blobs, which were placed in the upper portion of the tank. The bottom of the tank was filled with relatively low hydraulic conductivity $\left(K = 1.0 \times 10^{-6}\mathrm{m/s}\right)$ fine-grained industrial quartz sand to a height of 24 cm. Relatively high hydraulic conductivity $\left(K = 5.5 \times 10^{-3}\mathrm{m/s}\right)$ quartz-dominated sand was used to build up the remaining aquifer. The bulk aquifer porosity was 0.39. The dimensions of the rectangular-shaped coal-tar pool were 250 cm in length, 100 cm in width, and a thickness of 3 cm. The initial mass of the coal-tar pool was 40 kg. The experiment was conducted under constant flow velocity of 1.7 m/d for the first 177 days, then the velocity was raised to 5.1 m/d for the next 42 days, then the velocity was lowered to 3.4 m/d

 DOI 10.1007/s10040-006-0144-y

for the next 21 days, after which the velocity was lowered again back to 1.7 m/d for the remaining 114 days. The total experimental time was 354 days. It should be noted that these flow velocities are assumed to apply for the upper high hydraulic conductivity sand stratum. The groundwater velocity of the bottom lower hydraulic conductivity stratum is calculated using the ratio of hydraulic conductivities of the two strata, which is estimated to be 0.018% of the upper-stratum groundwater velocity. This indicates that the bulk aquifer flow is in the upper stratum. In the experiment, groundwater was degassed to minimize biodegradation of the organic contaminants.

Table 1 shows the initial composition of the experimental coal tar and relevant physical and chemical properties of each identified compound. Note that only a small fraction of coal-tar components could be identified and quantified. Approximately 38.32% (wt%) of the coal tar were identified, 22.58% of the remaining 61.68% were soluble in cyclohexane, and 39.1% of the remaining 61.68% were not soluble in cyclohexane.

Dissolved contaminant concentrations were observed at seven locations (0.5, 1, 2, 3, 4, 6, and 8 cm from the pool/water interface) 5 cm before the end of the pool (see Fig. 1a). Additionally, the pool plume was monitored near the end of the aquifer by a monitoring plane consisting of nine equally spaced locations 2 cm above the aquifer base. The observed dissolved contaminant concentrations from this monitoring plane are not used in this paper.

Numerical solution

The two-dimensional governing partial differential Eq. (4) is solved numerically using The alternating-direction-implicit, finite-difference time domain (ADI-FDTD) scheme. It should be noted that the numerical model presented in this study incorporates some of the unique phenomena of coal-tar dissolution, and is an enhanced version of the model presented by Lee and Chrysikopoulos (1998). Discretization of Eq. (4) results in a system of algebraic equations. This system of equations is solved using the mathematical computational software MATLAB. The spatial nodal separation distances are Δx=0.5 cm and Δz=0.2 cm, and the temporal separation duration is Δt=1 h. Figure 1b illustrates the numerical domain with boundary conditions for a stratified porous medium. Note that each sand

Table 1 Physical and chemical properties of identified coal-tar components

Compound	C^s (mg/L)[a]	$C^w(0)$ (mg/L)[a]	$\frac{f^S}{f^L}$ [a, b]	Log $K_{oc}^{b,c}$	Coal tar wt%[a]	D (cm^2/h)[d]
Benzene	1780	3.223	1	1.92	0.0950	0.0370
Toluene	534.8	1.586	1	2.49	0.1074	0.0328
Ethylbenzene	161.2	0.014	1	1.98	0.0044	0.0296
P-xylene	198	0.506	1	2.53	0.0692	0.0296
O-xylene	175	0.194	1	2.34	0.0251	0.0296
Propylbenzene	55	0.00028	1	3.45	0.0006	0.0237
1,2,4-Trimethylbenzene	59	0.054	1	3.63	0.0235	0.0237
1,2,3-Trimethylbenzene	75.2	0.015	1	3.63	0.0061	0.0237
1,3,5-Trimethylbenzene	48.2	0.025	1	3.63	0.0125	0.0237
Benzofuran	678	1.132	1	2.67	0.0913	0.0282
Indane	109.1	0.025	1	3.24	0.0090	0.0292
Indene	332.4	5.997	1	3.24	1.0648	0.0263
Naphthalene	31.7	26.52	0.3	2.97	14.09	0.0287
2-Methylnaphthalene	25.4	0.842	0.86	3.40	1.61	0.0264
1-Methylnaphthalene	28.045	0.393	1	3.36	0.69	0.0265
Acenaphthylene	9.804	1.048	0.22	3.59	1.99	0.0268
Acenaphthene	3.93	0.096	0.2	3.59	0.31	0.0262
Fluorene	1.98	0.263	0.16	4.15	1.69	0.0229
Phenanthrene	1.18	0.253	0.28	4.08	5.51	0.0241
Anthracene	0.05	0.049	0.01	4.20	1.35	0.0242
Fluoranthene	0.26	0.035	0.21	4.00	2.95	0.0229
Pyrene	0.13	0.024	0.11	4.22	2.13	0.0231
Benz(a)anthracene	0.014	0.0021	0.04	5.30	1.08	0.0212
Chrysene	0.002	0.0016	0.0097	4.00	0.76	0.0210
Benzo(b)fluoranthene	0.00323	0.0013[e]	0.039	5.74	1.17	0.0202
Benzo(k)fluoranthene	0.00055	–	0.013	–	–	–
Benz(a)pyrene	0.0038	0.00069	0.03	5.48	0.74	0.0204
Indeno(1,2,3-cd)pyrene	0.062	0.00019	0.0451	6.22	0.40	0.0196
Dibenz(a,h)anthracene	0.0005	0.000036	0.004	2.68	0.07	0.0189
Benzo(g,h,i)perylene	0.00026	0.00015	0.003	2.68	0.27	0.0198

[a] Eberhardt and Grathwohl (2002)

[b] Lee (2004)

[c] Sverdrup et al. (2002)

[d] Hayduk and Laudie (1974)

[e] Sum of benzo(b)fluoranthene and benzo(k)fluoranthene

 DOI 10.1007/s10040-006-0144-y

stratum is assumed homogeneous. Also, note that a matching flux boundary condition is used at the interface between the two sand strata (Lee and Chrysikopoulos 1998). In Fig. 1b, D_e^{T} and D_e^{B} represent the effective molecular diffusion in the upper and bottom stratum, respectively. The initial condition is $C_p(0,x,z)=0$.

Estimation of solute transport parameters

The molecular diffusion coefficient of each component in water is estimated using the Hayduk and Laudie (1974) correlation, and they are calculated using a water temperature of 25°C. The retardation factor for each component is estimated based on a linear isotherm with instantaneous, reversible sorption (Hashimoto et al. 1964)

$$R_p = 1 + \frac{\rho_{\mathrm{b}}}{\theta} K_{\mathrm{d}_p} \tag{5}$$

where ρ_{b} is the aquifer bulk density and K_{d} is the distribution coefficient estimated using the relationship $K_{\mathrm{d}_p} = f_{\mathrm{oc}} K_{\mathrm{oc}_p}$ (Karickhoff 1984), where f_{oc} is the organic carbon fraction of the porous medium and K_{oc} is the organic-carbon partitioning coefficient. Khodadoust et al. (2005) conducted sediment adsorption experiments using several PAH compounds and observed linear adsorption isotherms for all studied PAH compounds. For most coal-tar components, the values of K_{oc} are readily available in literature. However, the organic-carbon partitioning-coefficient values are not available for some PAH compounds and for those compounds the K_{oc} values are estimated using a correlation presented by Sverdrup et al. (2002). The correlation of Sverdrup et al. (2002) is based on the relationship between the octanol-water partitioning coefficient and the organic-carbon partitioning coefficient for eight PAH compounds. It should be noted that for some coal-tar constituents such as asphaltenes, its sorption onto sediments may be a temporally varying process (Dong et al. 2004). Furthermore, Eq. (5) assumes that sorption of each component is an independent process. However, due to the extensive number of dissolving compounds in a typical coal tar, more research is needed to verify this assumption.

The aquifer bulk density, organic-carbon fraction, and aquifer tortuosity used in this work take on assumed values of ρ_{b}=1.61 g/cm^3, f_{oc}=6.35×10^{-4}, and τ^*=1.41 for both strata (de Marsily 1986; Chrysikopoulos et al. 2000). Furthermore, the thin coal-tar pool is assumed homogeneous, which implies that diffusion of each component within the coal tar is rapid relative to the pool dissolution rate. However, resistance to dissolution of PAH compounds in the organic phase has been observed (Ortiz et al. 1999).

Model simulations and discussion

The objective of the simulations is to describe multicomponent contaminant transport within the experimental

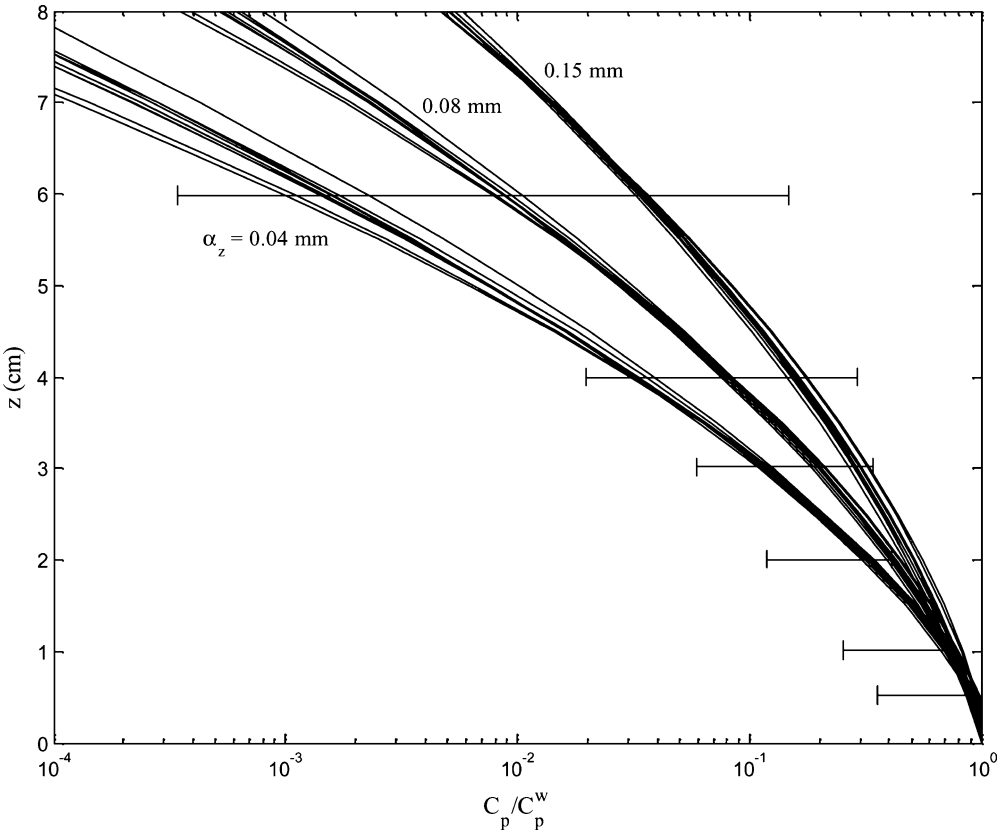

Fig. 2 Comparison between experimentally observed and simulated dissolved contaminant concentrations of ten coal-tar components using three different values of α_z: 0.04, 0.08, 0.15. The *horizontal lines* represent the range of observed coal-tar concentrations at various depths 5 cm before the edge of the pool

DOI 10.1007/s10040-006-0144-y

aquifer to a time of 354 days. The initial equilibrium aqueous solubility was observed for each of the identified coal-tar components and the values of $C_p^w(0)$ are listed in Table 1. Eberhardt and Grathwohl (2002) noted that no changes in dissolution rates were observed within the experimental time frame. Therefore, it is assumed that the equilibrium saturation concentration for each identified component remained constant until 354 days. As noted earlier, only 38.32% (wt%) of the experimental coal tar could be identified. Additionally, without knowledge regarding the comprehensive composition of the coal tar, Eqs. (2) and (3) cannot be used to estimate temporal changes in equilibrium aqueous solubility of each component. Consequently, this study is unable to simulate coal-tar dissolution for times past 354 days. The reader is referred to the work of Lee (2004) for long-term contaminant transport simulations resulting from dissolution of a well-defined coal-tar pool.

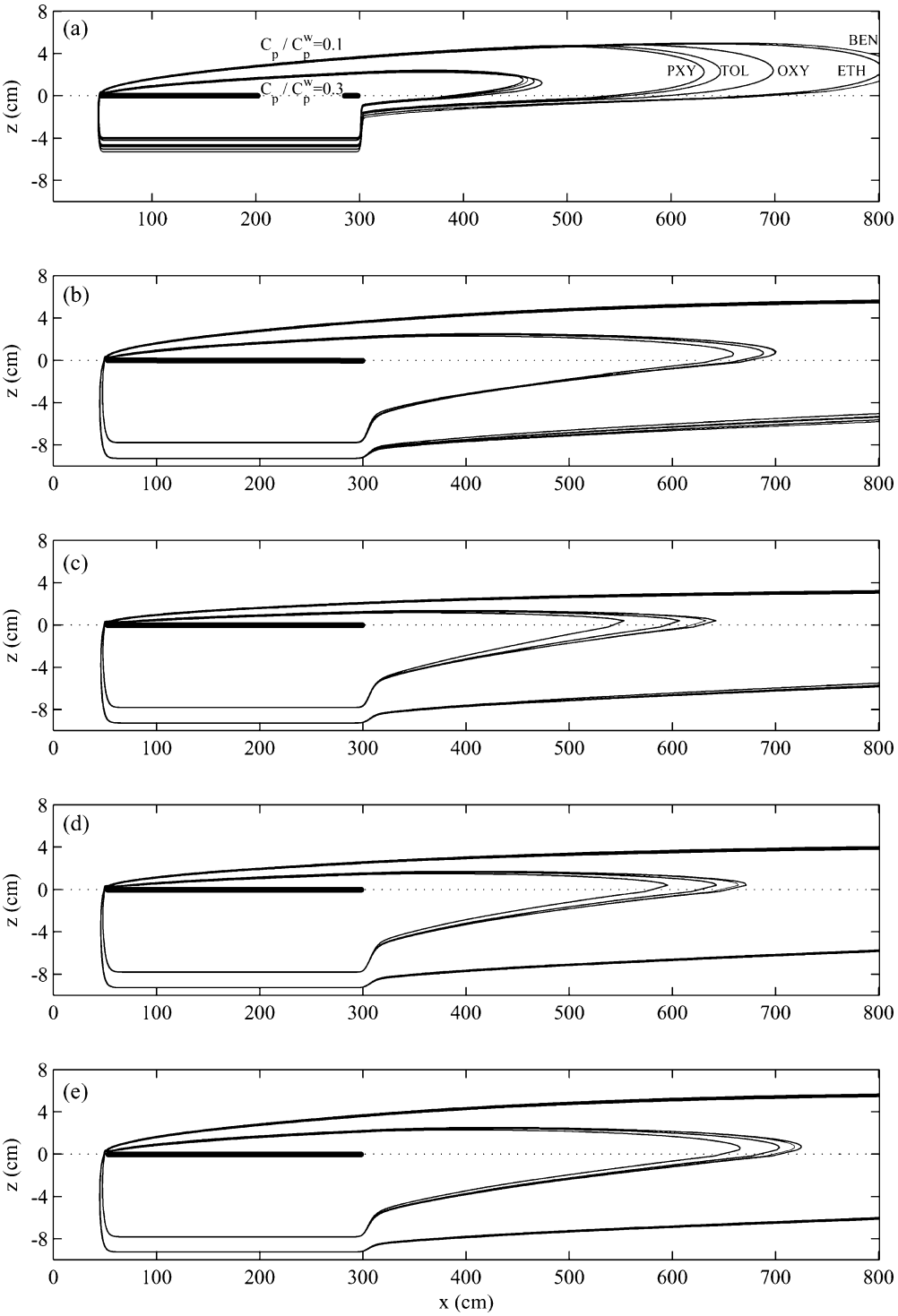

Fig. 3 Simulated dissolved contaminant concentration contours down the centerline of the experimental aquifer at **a** 5, **b** 170, **c** 210, **d** 240, and **e** 350 days since the initiation of the dissolution experiment for BTEX compounds. The *outer group of concentration contours* indicates $C_p(t)/C_p^w(0) = 0.1$ and the *inner group of contours* indicates $C_p(t)/C_p^w(0) = 0.3$

 DOI 10.1007/s10040-006-0144-y

Figure 2 shows the comparison between experimentally observed dissolved contaminant concentrations of ten coal-tar components and model-simulated concentrations of these identical components using three different α_z values. The ten coal-tar components are: benzene, toluene, ethylbenzene, p-xylene, o-xylene, indane, indene, 1,3,5-trimethylbenzene, 1,2,4-trimethylbenzene, and benzofuran. The horizontal straight lines represent the range of the observed contaminant concentrations at various depths 5 cm before the edge of the pool. The concentrations were observed between 36 to 87 days since initiation of the experiment. The solid lines represent the simulated dissolved concentration profiles at t=87 days. The groundwater velocity was 1.7 m/d during this time frame. Note that Fig. 2 shows three distinctive groups of simulated concentration profiles. The left-most group of concentration profiles is simulated using a vertical dispersivity of α_z=0.04 mm, the middle group of concentration profiles is

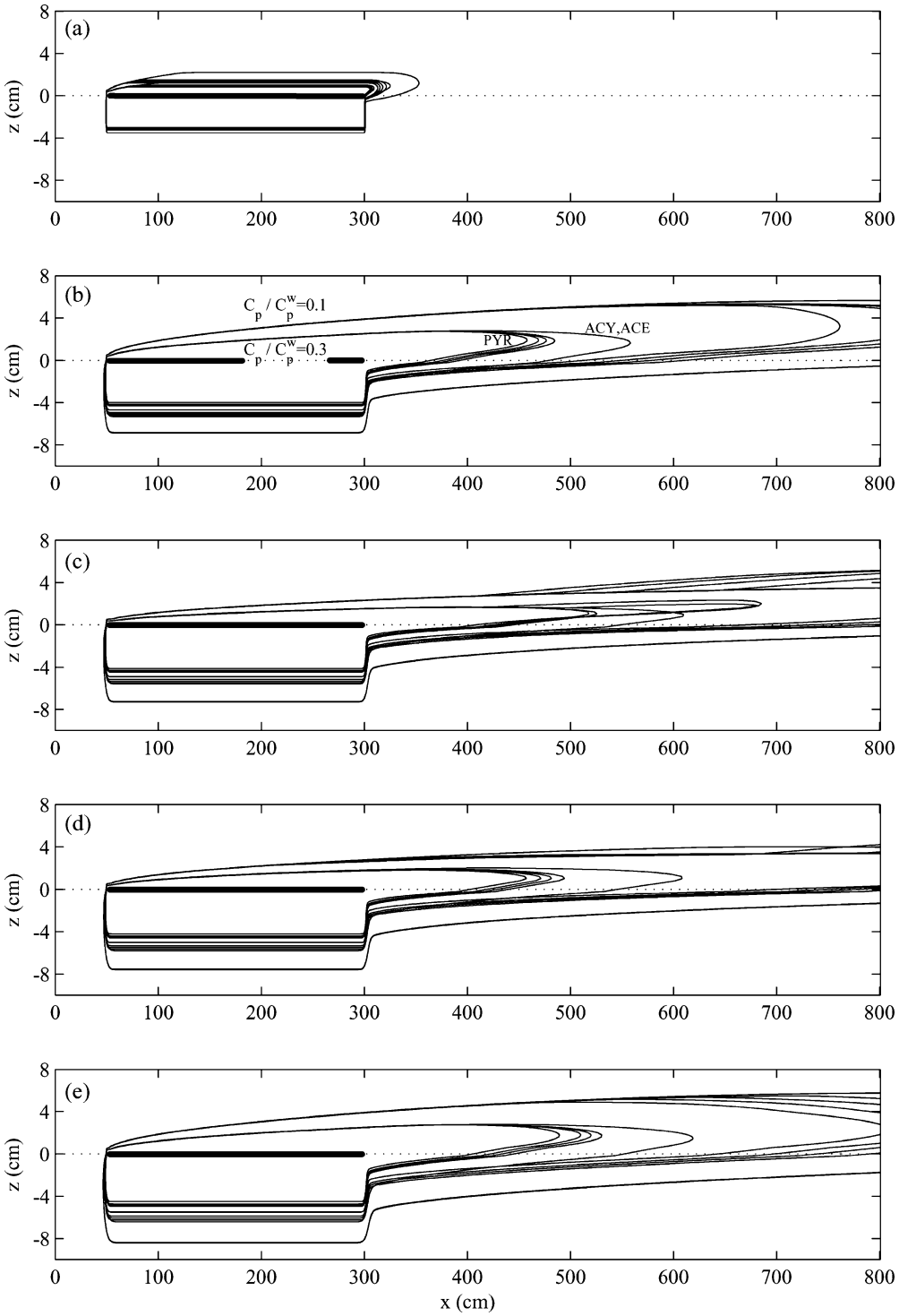

Fig. 4 Simulated dissolved contaminant concentration contours down the centerline of the experimental aquifer at **a** 5, **b** 170, **c** 210, **d** 240, and **e** 350 days since the initiation of the dissolution experiment for a group of PAH compounds with similar toxicity equivalent factors relative to benzo(a)pyrene. The *outer group of concentration contours* indicates $C_p(t)/C_p^w(0) = 0.1$ and the *inner group of contours* indicates $C_p(t)/C_p^w(0) = 0.3$. *PYR* pyrene; *FLN* fluoranthene; *PHN* phenanthrene; *FLR* fluorene; *ACY* acenaphthylene; *ACE* acenaphthene

 DOI 10.1007/s10040-006-0144-y

simulated using α_z=0.08 mm, and the right-most group of concentration profiles is simulated using α_z=0.15 mm. According to Fig. 2, a range of α_z values can be selected for simulation. It should be noted that there exists a wide variety of correlations between α_z and α_x in the literature. In this two-dimensional numerical study, a value of α_z=0.08 mm is selected for subsequent model simulations and the value of α_x is assumed to be ten times the value of α_z. It should also be noted that in this study, the presence of the low hydraulic conductivity bottom stratum does not effect concentrations observed at these sampling locations, which are in the upper stratum directly above the coal-tar pool.

As noted earlier, environmental scientists and engineers might especially be interested in the fate and transport of a few selected, or a group of dissolved coal-tar components. Figure 3a–e shows the simulated dissolved contaminant concentration contours down the centerline of the aquifer at 5, 170, 210, 240, and 350 days since initiation of the experiment for BTEX compounds. Figure 4a–e shows the simulated dissolved contaminant concentration contours down the centerline of the aquifer at 5, 170, 210, 240, and 350 days since initiation of the experiment for a group of PAH compounds consisting of (in order of increasing contour concentrations from left to right) pyrene (PYR), fluoranthene (FLN), phenanthrene (PHN), fluorene (FLR), acenaphthylene (ACY), and acenaphthene (ACE). Due to space limitations, contours of FLN, PHN, and FLR are not labeled. Also note that the simulated contours are practically identical for ACY and ACE. This group of PAH compounds has similar toxicity equivalent factors relative to benzo(a)pyrene, and might be of special interest in determining groundwater quality impacts (Dabestani and Ivanov 1999). The simulation times in Figs. 3 and 4 are selected based on the experimental groundwater velocity variations. The corresponding groundwater velocities for Figs. 3a–e and 4a–e are 1.7, 1.7, 5.1, 3.4, and 1.7 m/d. Each graph in Figs. 3 and 4 shows two distinctive groups of contours. The outer group of contours represents $C_p(t)/C_p^w(0) = 0.1$ and the inner group of contours represents $C_p(t)/C_p^w(0) = 0.3$. The coal-tar pool in Figs. 3 and 4 is located between $50 \leq x \leq 300$ cm, with a pool thickness of 3 cm in the $-z$ direction. The BTEX compounds in Fig. 3 have lower retardation as compared to the PAH compounds in Fig. 4. Therefore, it is expected that dissolved BTEX compounds would migrate faster in the aquifer, and this is apparent by comparing Figs. 3a and 4a. As evident in Figs. 3 and 4, diffusion plays a critical role in the transport of contaminants within the bottom stratum. Note that dissolved contaminants have migrated deeper in the $-z$ direction below the pool as compared to above the pool; and, due to higher retardation and lower molecular diffusion of PAH compounds (see Table 1), dissolved PAH compounds do not migrate as deep in the $-z$ direction as compared to BTEX compounds. Nevertheless, in a real case scenario where the subsurface formation is made up of multiple strata, dissolved contaminants below the pool may eventually migrate into and contaminate a deeper water-bearing stratum.

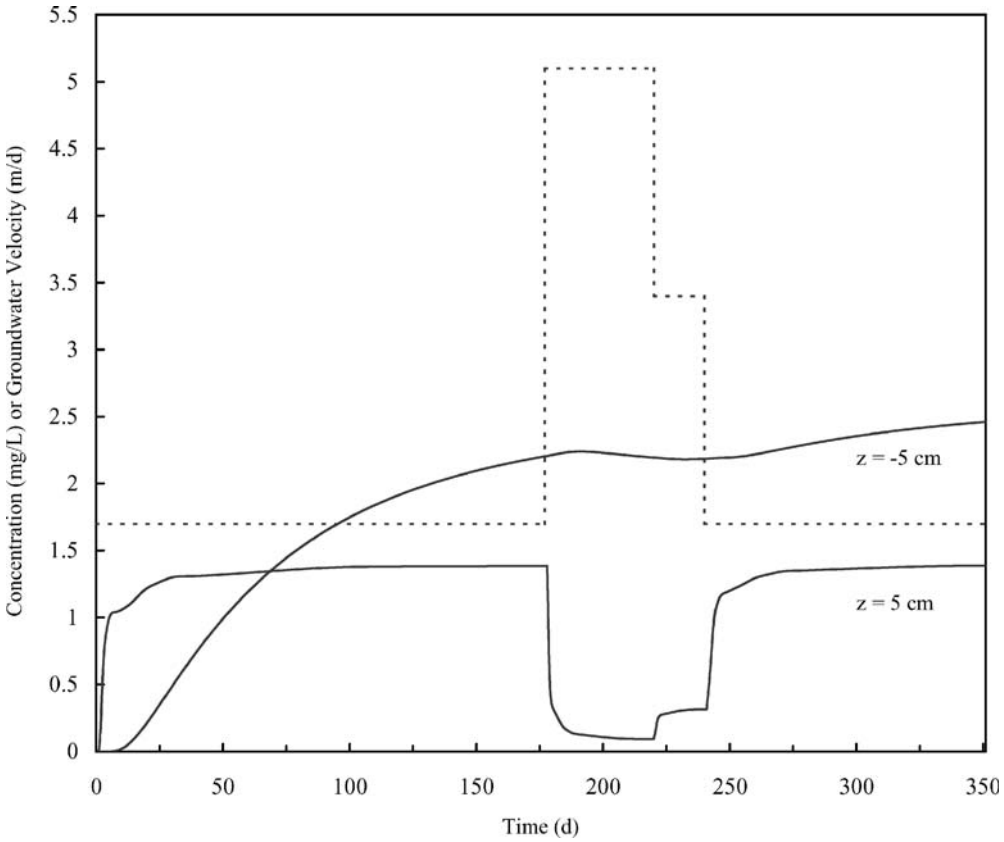

Fig. 5 The *solid lines* represent the summation concentration from all identified dissolved coal-tar components as a function of time at locations x=500 cm, z=5 cm, and x=500 cm, z=−5 cm, respectively. The *dotted line* represents the experimental groundwater velocity as a function of time

 DOI 10.1007/s10040-006-0144-y

Figure 5 shows the comparison of simulated dissolved concentrations (summation from all identified coal-tar components) as a function of time at two locations within the experimental aquifer. The first location is in the upper stratum at x=500 cm, z=5 cm, and the second location is in the bottom stratum at x=500 cm, z=−5 cm. The dotted line represents the experimental groundwater velocity as a function of time. It is interesting to note that two distinctive concentration profiles are generated despite the fact that the two locations are merely 10 cm apart in the z direction. Note that the coal-tar concentrations at this location (x=500 cm) in the bottom stratum are higher than in the upper stratum after approximately 70 days and remain higher despite changes in groundwater velocity. The influence of groundwater velocity variation on dissolved coal-tar concentrations is more apparent in the upper stratum as compared to the lower stratum; and, unlike the upper stratum, it does not appear that concentrations at this location (x=500 cm) in the lower stratum reached quasi steady-state under any velocity during the 354 days. If given the scenario that the coal-tar pool is removed at 354 days, aquifer contamination would continue for quite some time due to back diffusion of contaminants from the bottom stratum to the upper stratum.

Summary

In this study, a previously developed two-dimensional multicomponent numerical contaminant transport model is further developed for simulating the transport of dissolved contaminants originating from a coal-tar pool in a stratified, saturated porous medium. The model is used to simulate contaminant transport resulting from dissolution of a coal-tar pool in a rectangular-shaped large-scale experimental aquifer conducted by Eberhardt and Grathwohl (2002). The experiment was carried out to 354 days and the groundwater velocity was changed several times within this duration. Model simulations show good agreement against the experimentally observed dissolved contaminant concentrations. Next, the numerical model is used to simulate multicomponent contaminant plume evolution within the experimental aquifer. Results show that the transport characteristics among dissolved coal-tar components vary significantly. Furthermore, for a coal-tar pool trapped on top of a low hydraulic conductivity stratum, migration of solutes below the pool may eventually reach and contaminate a deeper water-bearing stratum.

Notation

The following symbols are used in this paper:

A	pool/water interfacial area (L^2)
C^s	aqueous saturation concentration ($M\ L^{-3}$)
C^w	equilibrium aqueous solubility ($M\ L^{-3}$)
d	coal-tar pool thickness (L)
D	molecular diffusion coefficient ($L^2\ T^{-1}$)
D_x	longitudinal hydrodynamic dispersion coefficient ($L^2\ T^{-1}$)
D_z	hydrodynamic dispersion coefficient in the vertical direction ($L^2\ T^{-1}$)
D_e	effective molecular diffusion coefficient ($L^2\ T^{-1}$)
f_{oc}	organic carbon fraction of the porous medium
f^S/f^L	solid to liquid reference fugacity ratio
$\overline{k}^T, \overline{k}^B$	average (or overall) mass transfer coefficient for the top and bottom pool/water interface, respectively ($L\ T^{-1}$)
K	hydraulic conductivity ($L\ T^{-1}$)
K_d	distribution coefficient ($L^3\ M^{-1}$)
K_{oc}	organic carbon partition coefficient ($L^3\ M^{-1}$)
M	number of moles (mol)
p	component number indicator
P	total number of components
R	dimensionless retardation factor
t	time (T)
U_x	average interstitial velocity ($L\ T^{-1}$)
V	coal-tar pool volume (L^3)
x,z	spatial coordinates (L)
X	nonaqueous phase mole fraction
α_x, α_z	longitudinal and transverse dispersivity, respectively (L)
Δt	numerical time step (T)
$\Delta x, \Delta z$	numerical nodal separation distance in the x and z directions, respectively (L)
θ	porosity (liquid volume/aquifer volume) ($L^3\ L^{-3}$)
λ	decay coefficient (T^{-1})
ρ	coal-tar component density ($M\ L^{-3}$)
ρ_b	sand bulk density ($M\ L^{-3}$)
τ^*	tortuosity factor (≥ 1)

Acknowledgments This study was partially funded by a research grant from the West Virginia University Institute of Technology Foundation. The authors would like to thank Ms. Jessica Kruczek for contributing to the simulations.

References

Brown DG, Knightes CD, Peters CA (1999) Risk assessment for polycyclic aromatic hydrocarbon NAPLs using component fractions. Environ Sci Technol 33:4357–4363

Chrysikopoulos CV, Lee KY (1998) Contaminant transport resulting from multicomponent nonaqueous phase liquid pool dissolution in three-dimensional subsurface formations. J Contam Hydrol 31:1–21

Chrysikopoulos CV, Lee KY, Harmon TC (2000) Dissolution of a well-defined trichloroethylene pool in saturated porous media: experimental design and aquifer characterization. Water Resour Res 36:1687–1696

Dabestani R, Ivanov IN (1999) A compilation of physical, spectroscopic and photophysical properties of polycyclic aromatic hydrocarbons. Photochem Photobiol 70:10–34

de Marsily G (1986) Quantitative hydrogeology, groundwater hydrology for engineers. Academic Press, San Diego, CA

Dong J, Chowdhry B, Leharne S (2004) Investigation of the wetting behavior of coal tar in three phase systems and its modification by poloxamine block copolymeric surfactants. Environ Sci Technol 38:594–602

 DOI 10.1007/s10040-006-0144-y

Eberhardt C, Grathwohl P (2002) Time scales of organic contaminant dissolution from complex source zones: coal tar pools vs. blobs. J Contam Hydrol 59:45–66

Hashimoto I, Deshpande KB, Thomas HC (1964) Peclet numbers and retardation factors for ion exchange columns. Ind Engr Chem Fund 3:213–218

Hayduk W, Laudie H (1974) Prediction of diffusion coefficients for nonelectrolytes in dilute aqueous solutions. AIChE J 20:611–615

Karickhoff SW (1984) Organic pollutant sorption in aquatic systems. J Hydraul Eng ASCE 110:707–735

Khodadoust AP, Lei L, Antia JE, Bagchi R, Suidan MT, Tabak HH (2005) Adsorption of polycyclic aromatic hydrocarbons in aged harbor sediments. J Environ Eng ASCE 131:403–409

King MWG, Barker JF (1999) Migration and natural fate of a coal tar creosote plume. 1. Overview and plume development. J Contam Hydrol 39:249–279

Lee KY (2004) Modeling long-term transport of contaminants resulting from dissolution of a coal tar pool in saturated porous media. J Environ Eng ASCE 130:1507–1513

Lee KY, Chrysikopoulos CV (1998) NAPL pool dissolution in stratified and anisotropic porous formations. J Environ Eng ASCE 124:851–862

Lee KY, Chrysikopoulos CV (2006) Dissolution of a multicomponent DNAPL pool in an experimental aquifer. J Hazard Mater B128:218–226

Loibner AP, Szolar OHJ, Braun R, Hirmann D (2004) Toxicity testing of 16 priority polycyclic aromatic hydrocarbons using Lumistox. Environ Toxicol Chem 23:557–564

Mueller JG, Chapman PJ, Pritchard PH (1989) Creosote-contaminated sites: their potential for bioremediation. Environ Sci Technol 23:1197–1201

Ortiz E, Kraatz M, Luthy RG (1999) Organic phase resistance to dissolution of polycyclic aromatic hydrocarbon compounds. Environ Sci Technol 33:235–242

Peters CA, Mukherji S, Knightes CD, Weber WJ (1997) Phase stability of multicomponent NAPLs containing PAHs. Environ Sci Technol 31:2540–2546

Sverdrup LE, Nielsen T, Krogh PH (2002) Soil ecotoxicity of polycyclic aromatic hydrocarbons in relation to soil sorption, lipophilicity, and water solubility. Environ Sci Technol 36:2429–2435

Tiruta-Barna L, Mahjoub B, Faure L, Hanna K, Bayard R, Gourdon R (2006) Assessment of the multi-compound non-equilibrium dissolution behavior of a coal tar containing PAHs and phenols into water. J Hazard Mater B132:277–286

 DOI 10.1007/s10040-006-0144-y